



Trans. Nonferrous Met. Soc. China 31(2021) 3328-3341

Transactions of Nonferrous Metals Society of China

www.tnmsc.cn



# Theoretical design and distribution control of precipitates and solute elements in Al–Zn–Mg–Cu alloys with heterostructure

Liang-liang YUAN<sup>1</sup>, Ming-xing GUO<sup>1,2</sup>, Yong YAN<sup>3,4</sup>, Wei-jun FENG<sup>3,4</sup>, Zan-yang LIU<sup>1</sup>, Lin-zhong ZHUANG<sup>1,2</sup>

1. State Key Laboratory for Advanced Metals and Materials,

University of Science and Technology Beijing, Beijing 100083, China;

2. Beijing Laboratory of Metallic Materials and Processing for Modern Transportation,

University of Science and Technology Beijing, Beijing 100083, China; 3. Baowu Aluminum Technical Center, Baosteel Central Research Institute,

Baoshan Iron & Steel Co., Ltd., Shanghai 201900, China;

4. Sanmenxia Aluminum-based New Material R&D Center, China Baowu Steel Group, Sanmenxia 472099, China

Received 13 September 2021; accepted 7 November 2021

**Abstract:** In order to simultaneously improve strength and formability, an analytical model for the concentration distribution of precipitates and solute elements is established and used to theoretically design and control the heterogeneous microstructure of Al–Zn–Mg–Cu alloys. The results show that the dissolution of precipitates is mainly affected by particle size and heat treatment temperature, the heterogeneous distribution level of solute elements diffused in the alloy matrix mainly depends on the grain size, while the heat treatment temperature only has an obvious effect on the concentration distribution in the larger grains, and the experimental results of Al–Zn–Mg–Cu alloy are in good agreement with the theoretical model predictions of precipitates and solute element concentration distribution. Controlling the concentration distribution of precipitates and solute elements in Al–Zn–Mg–Cu alloys is the premise of accurately constructing heterogeneous microstructure in micro-domains, which can be used to significantly improve the formability of Al–Zn–Mg–Cu alloys with a heterostructure.

Key words: Al-Zn-Mg-Cu alloys; concentration distribution; diffusion; heterogeneous microstructure; model

#### 1 Introduction

Heat-treatable and age-hardening characteristics make Al-Zn-Mg-Cu alloys a very attractive automotive structural material [1-4], which are expected to replace steel structural parts to avoid aluminum-steel welding, corrosion and other problems, and can significantly improve the lightweight of automobiles.

The thermomechanical processing of Al alloy sheets for automobile, normally includes, casting  $\rightarrow$  homogenization  $\rightarrow$  hot rolling  $\rightarrow$  cold rolling  $\rightarrow$ 

intermediate annealing  $\rightarrow$  cold rolling  $\rightarrow$  solid solution treatment  $\rightarrow$  pre-aging  $\rightarrow$  stamping, and so on [5]. A reasonable heat treatment process, such as, the selection of heat treatment temperature and time, not only can affect the microstructure and properties of the alloys, but also can play a significant role in controlling the industrial production cost of the alloys.

During the heat treatments of alloys, the precipitates in the alloys can be dissolved, and the solute concentration gradient in the matrix can be changed through solute diffusion, which determines the size, morphology, number density

and distribution of the precipitates and further leads to the concentration redistribution of solute elements in the alloys [6-10]. After subsequent thermomechanical treatment, such as solid solution and artificial aging, a large number of precipitates can be formed in the alloys to enhance the strengths. For instance, the metastable nano-sized precipitates  $\eta'$  are the main strengthening phases in the Al-Zn-Mg-Cu alloys. Through different aging processes controlling, the strength, corrosion resistance and toughness of the alloys can be greatly improved to the high levels. However, when the alloys exhibit ultra-high strength, their ductility and room temperature formability normally decrease significantly [11,12]. Therefore, how to make Al-Zn-Mg-Cu alloys have both high strength and high formability through microstructure design and thermomechanical processing controlling is of great significance to their wide applications.

Actually, it is a common problem to find a better way to make metal materials possess both high strength and high ductility [13-15]. For example, the increased strength of polycrystalline materials with nano-size grains prepared by traditional thermomechanical processing always leads to the decrease in ductility at the same time [16-18], in addition, high-entropy alloys and amorphous alloys also exhibit lower ductility due to their higher strength. In order to effectively improve the ductility of the above alloys, a large number of studies have shown that the design and control of the heterogeneous structure can be considered as a more effective method to improve the ductility of the alloys [19-24], such as, the formation of multi-scale structure, gradient grain structure, grain microstructure, bimodal and nanostructure. And then, the developed alloys with heterogeneous structure can possess both high strength and high ductility at the same time. Accordingly, if a special heterogeneous structure can be also designed and formed in the high strength Al-Zn-Mg-Cu alloys, the formability of the alloys should be greatly improved to meet the demanding requirements. However, up to date, there is no related literature on how to design and construct the heterogeneous microstructure of high strength 7xxx alloys. In order to solve this problem, this work considers how to better design and construct the heterogeneous microstructure, i.e.,

special co-existence distribution characteristics of hard and soft micro-domains, from the perspective of theoretical calculation, hoping to provide an important guidance for designing and controlling the heterostructure of high strength Al–Zn–Mg–Cu alloys, and play a key role in promoting the development of high strength and high formability Al–Zn–Mg–Cu alloys in the automotive field.

#### 2 Theoretical analysis model

The heat treatment process generally includes the dissolution of the second phase particles and the homogenization of the composition in the alloy matrix. If a homogenization treatment is used in an Al alloy in the as-cast state, the second phase particles in the alloy can be dissolved according to the phase equilibrium condition, and a diffusion field can be formed around the precipitates in the matrix due to the diffusion of solutes. Thus, a solute concentration gradient can be further formed in the alloy matrix in order to achieve the final homogeneous distribution of solutes [25]. Considering the fact that the diffusion rate is relatively slow, it is quite easy to establish a new equilibrium by the dissolution of the precipitates at the phase interface, which makes the diffusion of solute elements in the matrix a limiting link of the whole homogenization process. Thus, the dissolution process of the second phases is essentially controlled by solute diffusion in the matrix.

WHELAN [26] proposed a classical single-particle dissolution model based on the assumption that the interface between particles and matrix is a stationary interface, and then ZUO et al [27] further modified the model by combining with the JMA-like equation to deal with the interaction between adjacent particles, so that it can be approximately applied to the multicomponent alloy system. In this work, the dissolution process of precipitates in the Al–Zn–Mg–Cu alloy was also simulated by using this model, and the dissolution time is predicted accurately.

The schematic diagram of the dissolution of the second phase particles in the alloy and the concentration distribution curve of solute elements in the alloy matrix is shown in Fig. 1. It is assumed that all precipitates are of the same size, spherical and uniformly distributed at the grain boundary,

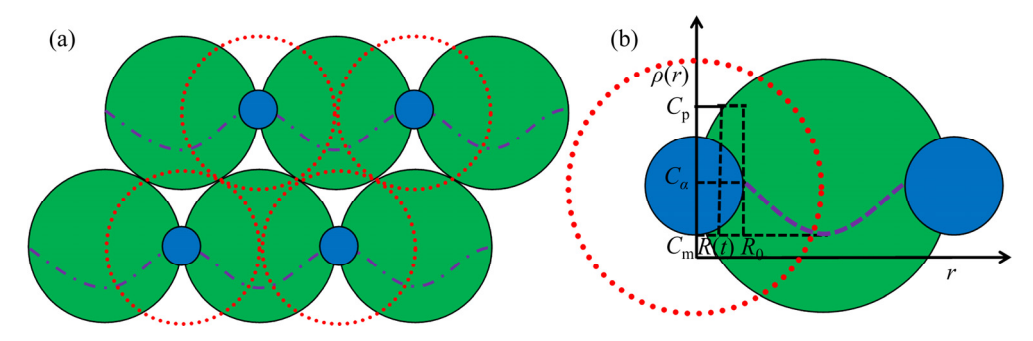


**Fig. 1** Schematic diagram of models showing grains, precipitates and solute concentration distribution curve of Al–Zn–Mg–Cu alloys: (a) Designed model; (b) Solute concentration profile

and the alloy is approximately regarded as being composed of many spherical grains of the same size. As shown in Fig. 1, the green sphere represents the grain, the blue sphere represents the precipitate located at boundary of grain, the red dotted line represents the diffusion field formed around the particles, and the purple line represents the concentration distribution curve in the matrix.

#### 2.1 Dissolution model of precipitates

Based on the assumption that the composition of the precipitates remains unchanged and the cross-diffusion coefficient of solute elements is zero in the dissolution process, the dissolution formula of a single spherical particle controlled by diffusion can be obtained as follows [26,28]:

$$\frac{\mathrm{d}R}{\mathrm{d}t} = -\frac{kD}{2R} - \frac{k}{2} \sqrt{\frac{D}{\pi t}} \tag{1}$$

$$D = D_0 \exp\left(-\frac{Q}{R_{\rm g}T}\right) \tag{2}$$

where R is the radius of spherical precipitated particles, k is the concentration constant, D is the diffusion coefficient, t is the dissolution time, T is the temperature,  $R_{\rm g}$  is the gas constant,  $D_0$  is the pre-exponential factor of diffusion, and Q is the activation energy of diffusion.

$$k = \frac{2(C_{\alpha} - C_{\rm m})}{C_{\rm p} - C_{\alpha}} \tag{3}$$

where  $C_{\rm p}$  represents the concentration of elements in the precipitated particles,  $C_{\alpha}$  represents the concentration of elements at the interface between the particles and the matrix, which is equal to the atomic solid solubility of the element at the dissolution temperature, and  $C_{\rm m}$  represents the

concentration of elements in the matrix.

Then, the relationship between the radius R of the spherical precipitated particles and the dissolution time t can be expressed as [27]

$$R = \sqrt{\frac{k}{\pi}} (R_1 - \sqrt{kDt}) + \sqrt{R_1^2 - kDt}$$
 (4)

where  $R_1$  represents the decrease in the radius of spherical precipitates from the initial radius  $R_0$  to R(t), and  $R_1$  can be obtained,

$$R_{1} = \frac{1}{\left(1 + \sqrt{\frac{k}{\pi}}\right)} R_{0} \tag{5}$$

ZUO et al [27] dealt with the diffusioncontrolled dissolution transition in multi-particle systems by introducing JMA theory, which can be described as

$$f_t = 1 - \exp(-x_e) \tag{6}$$

where  $f_t$  represents the degree of dissolution of precipitated particles in the dissolution process, and  $x_e$  represents the volume fraction dissolved by ignoring the interaction between adjacent particles.

Then,  $x_e$  can be obtained,

$$x_e = \frac{V_0 - V}{V_0} = \frac{R_0^3 - R^3}{R_0^3} \tag{7}$$

where  $V_0$  represents the initial volume of the precipitated particles.

ZUO et al [27] and ZHANG et al [29] further modified the classical JMA model by introducing the proportional factor m, so that it can be used in the whole dissolution process. The modified transformation fraction  $f_{t_m}$  can be described as

$$f_{t_m} = m[1 - \exp(-x_e)] \tag{8}$$

Here,

$$m = \frac{e}{e - 1} \tag{9}$$

where e is a constant equals 2.718.

Accordingly, the relationship between the particle radius  $R_{t_m}$  at the modified transition time  $t_m$  and the initial radius of the particle can be expressed as

$$(R_t / R_0)^3 = 1 - f_t = 1 - m[1 - \exp(-x_e)]$$
 (10)

where  $x_e$  can be obtained by solving Eqs. (4), (7) and (8):

$$x_{e} = \frac{1}{R_{0}^{3}} \left\{ 3R_{0} \left[ \sqrt{\frac{k}{\pi}} \left( R_{1} - \sqrt{\frac{kDt_{m}}{m}} \right) + \sqrt{R_{1}^{2} - \frac{kDt_{m}}{m}} \right] \cdot \left( \frac{\sqrt{kDt_{m}}}{\sqrt{m}R_{1} + \sqrt{mR_{1}^{2} - kDt_{m}}} + \sqrt{\frac{k}{\pi}} \right) \cdot \left( \frac{kDt_{m}}{m} \right)^{1/2} + \left( \frac{\sqrt{kDt_{m}}}{\sqrt{m}R_{1} + \sqrt{mR_{1}^{2} - kDt_{m}}} + \sqrt{\frac{k}{\pi}} \right)^{3} \cdot \left( \frac{kDt_{m}}{m} \right)^{3/2} \right\}$$
(11)

## 2.2 Solute element concentration distribution model

Due to the dissolution behavior of the second phase particles, the solute elements around the particles form a concentration field with gradient distribution, and when the precipitated particles are completely dissolved, the concentration distribution of solute elements in the alloy matrix is still uneven, which leads to the composition homogenization process controlled by element diffusion.

Assuming that the concentration distribution of solute elements in the grains along the diameter direction conforms to the cosine wave, the concentration distribution in the grain C(x) is expressed as

$$C(x) = C_0 + (C_{\text{max}} - C_0) \cos\left(\frac{\pi x}{R_G}\right)$$
 (12)

where  $C_0$  represents the equilibrium concentration of solute elements, which is also the designed concentration of composition, x is the location of concentration change,  $C_{\text{max}}$  represents the maximum concentration of elements detected in the matrix, and  $R_{\text{G}}$  represents the grain radius. Driven by the concentration gradient, the solute elements continue to diffuse to equilibrium, i.e.,

$$C(x=0, t)=C_0$$
 (13)

$$\frac{\mathrm{d}C}{\mathrm{d}x}(x=\frac{R_{\mathrm{G}}}{2},\ t)=0\tag{14}$$

According to Fick's second law:

$$\frac{\partial C}{\partial t} = D \frac{\partial^2 C}{\partial x^2} \tag{15}$$

Equations (16)–(18) can be obtained by using the method of separated variables to solve the diffusion equation:

$$C(x, t) = X(x)T(t)$$
(16)

where X(x) is the variable of concentration position, and T(t) is the temperature related to time.

$$\frac{\mathrm{d}^2 X}{\mathrm{d}x^2} + \left(\frac{\pi}{R_{\mathrm{G}}}\right)^2 X = 0 \tag{17}$$

$$\frac{\mathrm{d}T}{\mathrm{d}t} + D\left(\frac{\pi}{R_{\rm G}}\right)^2 T = 0 \tag{18}$$

Combined with the boundary conditions described by Eqs. (13) and (14), the function of solute elements concentration in the alloy matrix with time and distance can be described as

$$C(x,t) = C_0 + (C_{\text{max}} - C_0) \cos\left(\frac{\pi x}{R_G}\right) \exp(-\pi^2 Dt / R_G^2)$$
(19)

#### 3 Results

The composition of the alloy used in this work Al-5Zn-1.5Mg-1.5Cu-0.2Fe-0.1Mn-0.1Ti-0.03Ni (wt.%). The microstructure of the alloy in the as-cast state was observed under scanning electron microscope (SEM), as shown in Fig. 2. The as-cast microstructure shows that the average grain size is about 100 μm, the precipitates are mainly distributed at the grain boundaries, which are composed of AlFeCu phase and AlZnMgCu phase, and a small amount of AlZnMgCu phases are distributed in the grains (as shown in Fig. 2). The specific composition of the precipitates was characterized by electron dispersive spectroscopy (EDS), and the results are reported in Figs. 2(d) and (e). Because AlFeCu is insoluble phase with high melting point, the dissolution of precipitates in the heat treatment process is only focused on the AlZnMgCu phase [30,31].

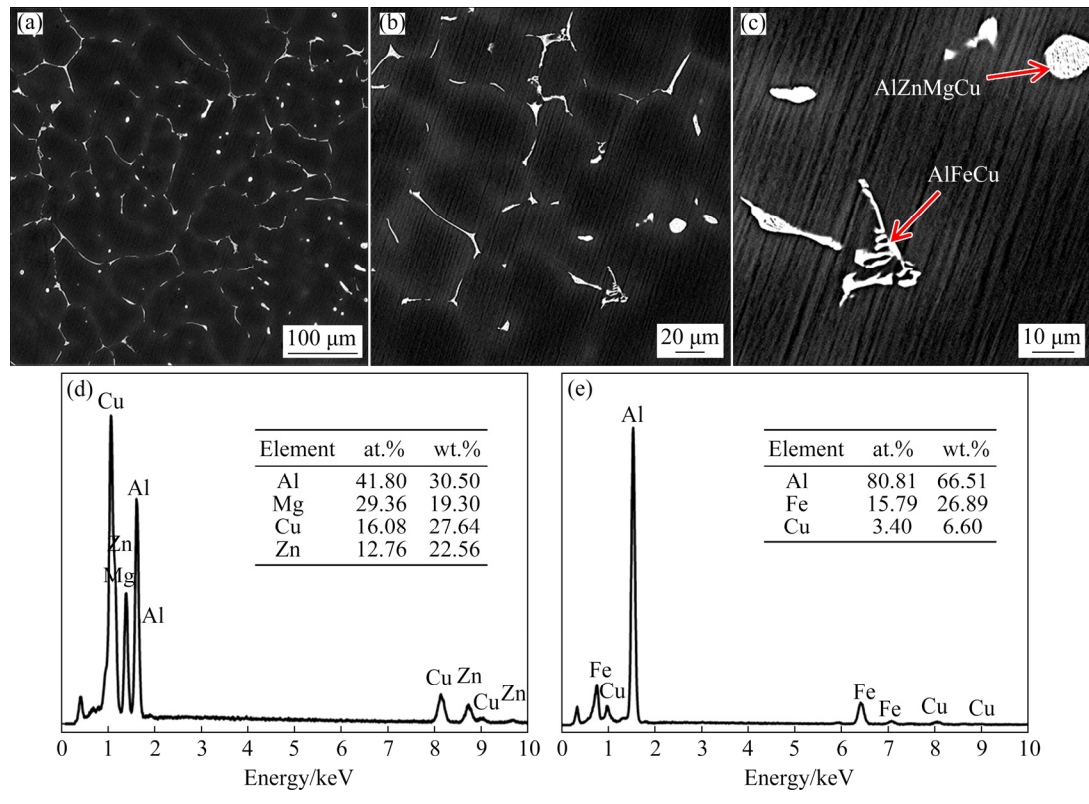


Fig. 2 Microstructures of Al–Zn–Mg–Cu alloy in as-cast state at low (a) and high (b, c) magnifications, and EDS maps of AlZnMgCu (d) and AlFeCu (e) phases

It has been pointed out in Ref. [32] that the diffusion of Cu element is obviously slower than that of Zn and Mg elements under the same conditions, which makes the diffusion of Cu element a limiting link in the diffusion process. Accordingly, the diffusion coefficients (*D*) of solute elements are compared, as shown in Table 1 [31,32]. It is found that the diffusion coefficients of Cu element are obviously lower than those of Zn and Mg elements in the heat treatment temperature range used in this paper, which is consistent with the reports in Ref. [33]. Therefore, in order to better highlight the functional relationship between the influencing factors and the diffusion curve, only the diffusion of Cu element is discussed in this work.

Based on the statistical analysis of the particle radius  $(R_0)$  of AlZnMgCu quaternary phase in the

**Table 1** Values of parameters used in model [31,32]

Element	$D_0$ /	Q/	$D_{ m 460^{\circ}C}/$	D <sub>475 °C</sub> /
	$(m^2 \cdot s^{-1})$	$(kJ{\cdot}mol^{-1})$	$(m^2 \cdot s^{-1})$	$(m^2 \cdot s^{-1})$
Zn	$1.19 \times 10^{-5}$	116.1	$6.348 \times 10^{-14}$	$9.301 \times 10^{-14}$
Mg	$1.49 \times 10^{-5}$	120.5	$3.862{\times}10^{-14}$	$5.741{\times}10^{-14}$
Cu	$4.44 \times 10^{-5}$	133.9	$1.274 \times 10^{-14}$	$1.979 \times 10^{-14}$

as-cast alloy, it is found that  $R_0$  is distributed between 3 and 10 µm, so the  $R_0$  values used in the model are 3, 4, 5, 6, 8 and 10 µm, respectively. According to the Factsage phase diagram, the atomic solid solubility  $C_{\alpha}$  of Cu element at different temperatures is calculated theoretically, as shown in Table 2. Accordingly, combined with Eqs. (2) and (3), k and D values at different temperatures can be obtained, which are also listed in Table 2.

Table 2 Parameter values of Cu element in model

Temperature/°C	$C_{\alpha}$ /%	k	$D/(\text{m}^2 \cdot \text{s}^{-1})$
460	2.24	0.2449	$1.274 \times 10^{-14}$
465	2.38	0.2623	$1.478 \times 10^{-14}$
470	2.73	0.3067	$1.712 \times 10^{-14}$
475	2.86	0.3237	$1.979 \times 10^{-14}$

EDS composition analysis is carried out in the as-cast grains, and a large number of composition results along the diameter and equal step length are summarized, as shown in Fig. 3, which well indicates the trend of concentration change in the grain unit. According to the EDS analysis on the solute distribution in the typical one of the many

selected as-cast grains (as presented in Fig. 3), it can be seen that a gradient concentration of solute elements has been formed in the grains.

With the increase of heat treatment time, the precipitates begin to be dissolved. Based on the model mentioned above assuming that the concentration of Cu element in the matrix is 0, the relationship between  $(R_{t_m}/R_0)^3$  and  $t_m$  with different particle sizes can be established according to Eq. (10), as shown in Fig. 4. It is obvious that the radius of the precipitated particles greatly affects the dissolution time of the precipitates at the same

temperature. As shown in Fig. 4(a), when the heat treatment temperature is 460 °C, the precipitated particles with a radius of 10  $\mu$ m need about 8 h to dissolve completely, while the particles with a radius of 5  $\mu$ m take only 2 h to fully dissolve.

In order to better show the effect of heat treatment temperature on the dissolution of precipitated particles, the typical particle radius was selected to calculate the dissolution curves of precipitated particles at different temperatures, as shown in Fig. 5. There is no doubt that the dissolution of precipitated particles increases with

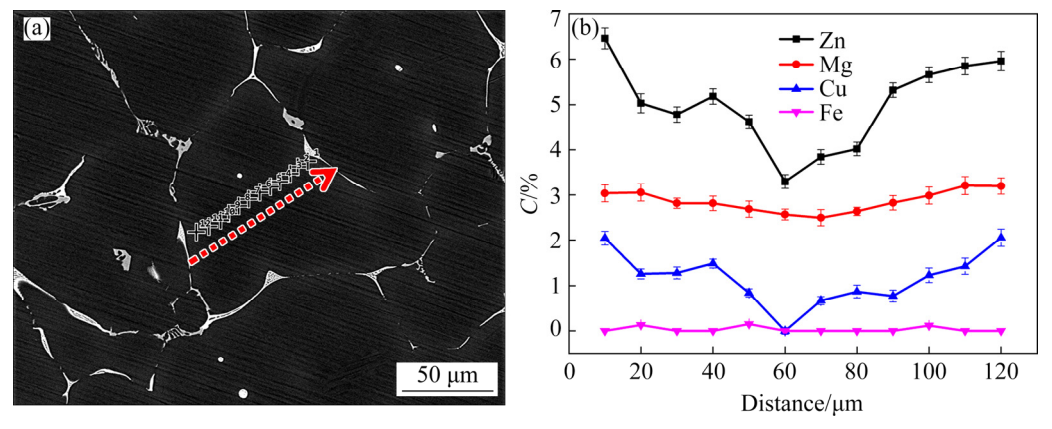


**Fig. 3** Microstructure and concentration (*C*) distribution of solute elements in as-cast grains: (a) SEM image; (b) Concentration distribution curves

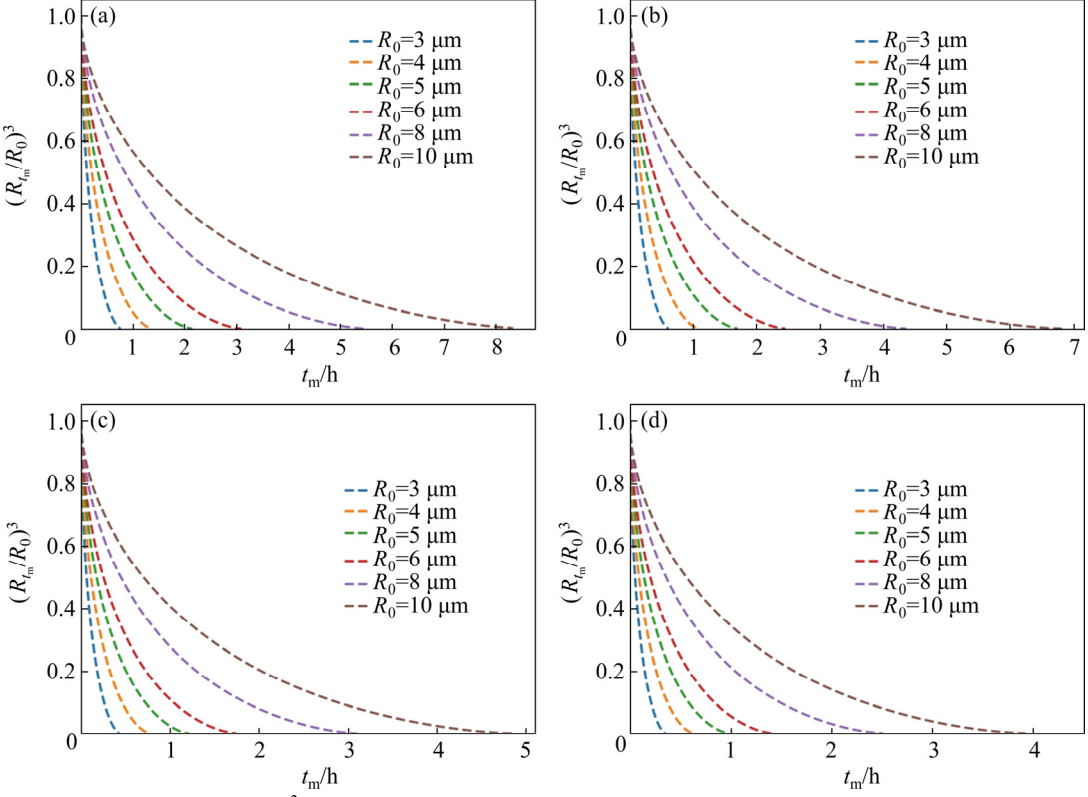


**Fig. 4** Relationship between  $(R_{t_m}/R_0)^3$  and  $t_m$  for Cu element in Al–Zn–Mg–Cu with different sizes ( $C_m$ =0) at 460 °C (a), 465 °C (b), 470 °C (c), and 475 °C (d)

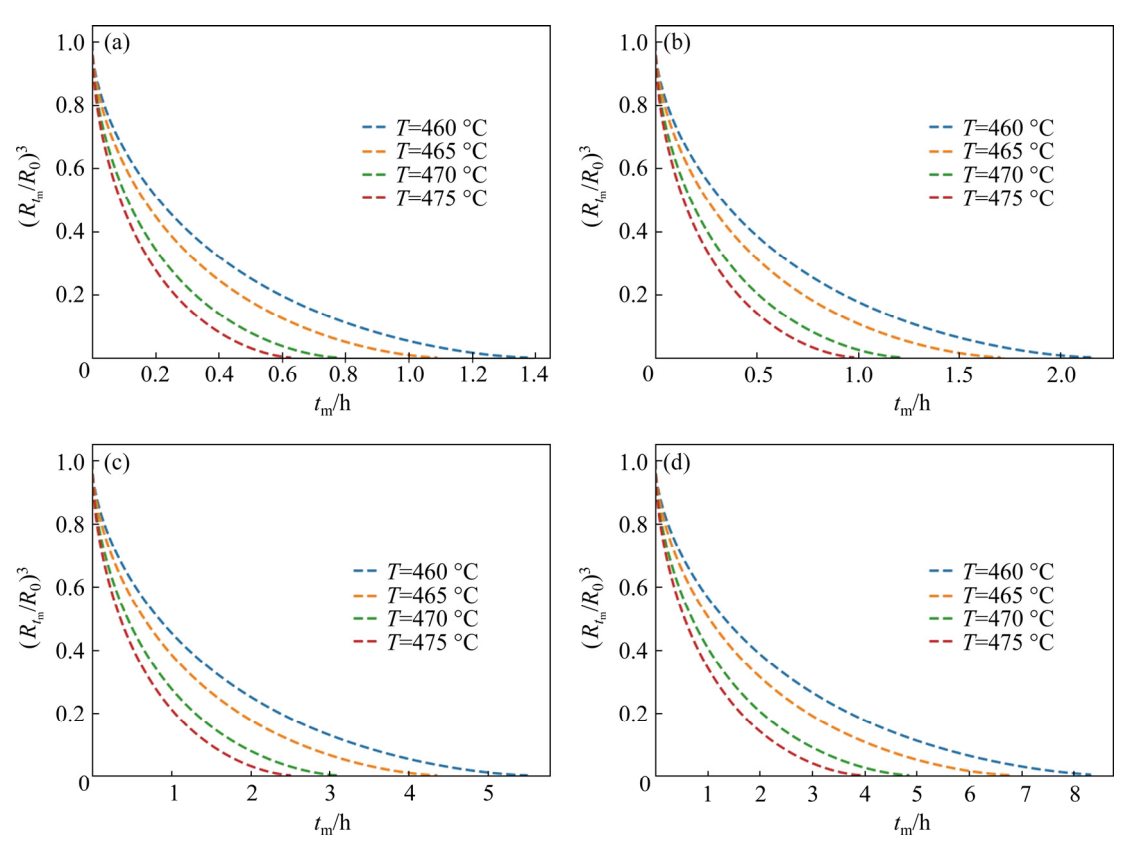


**Fig. 5** Relationship between  $(R_{t_m}/R_0)^3$  and  $t_m$  for Cu element in Al–Zn–Mg–Cu at different temperatures and  $R_0$ =4 μm  $(C_m$ =0) (a),  $R_0$ =5 μm (b),  $R_0$ =8 μm (c), and  $R_0$ =10 μm (d)

the increase of temperature. As shown in Fig. 5(d), when the heat treatment temperature increases from 460 to 475  $^{\circ}$ C, the dissolution time of precipitated particles with a radius of 10  $\mu$ m is shortened from 8 to 4 h, which proves that the increase in temperature significantly accelerates the dissolution of particles.

With the dissolution of precipitated particles, the diffusion homogenization of solute elements occurs in the alloy matrix at the same time. The diffusion field formed during the dissolution of precipitated particles has a certain concentration contribution to the homogenization of components in the matrix. When the precipitated particles are dissolved completely, it is necessary to identify the actual concentration distribution in the matrix in order to determine the initial concentration state of matrix homogenization that occurs in the following time. Accordingly, the maximum concentration distribution of solute element Cu in the alloy matrix  $C_{\rm max}$  is 2.5%. As mentioned above, the average grain size of the alloy is 100 µm and the equilibrium concentration of solute element Cu is 1.5%. When the maximum concentration in the matrix is 1.6%, 1.9%, 2.2%, and 2.5%, respectively, the concentration distribution in the matrix is discussed in detail. As shown in Fig. 6, there is no significant difference in the effect of the maximum concentration of solute element Cu in the matrix on the heat treatment time at the same heat treatment temperature.

In order to better highlight the distribution of solute concentration in the matrix along the diameter direction, the functional relations with time and distance are further calculated for different maximum concentrations. It is clear that the concentration on both sides of the grain is higher than that in the center of the grain due to the dissolution of the precipitates at the grain boundary. Figure 7 shows the concentration distribution curves of Cu element in the grain at 460 °C, which reveals that the concentration distribution tends to be uniform after heat treatment for about 15 h. With the continuous diffusion behavior, the concentration at the edge of grain decreases and the concentration in the center increases gradually, which finally leads to the homogenization of the concentration distribution of solute elements in the matrix.

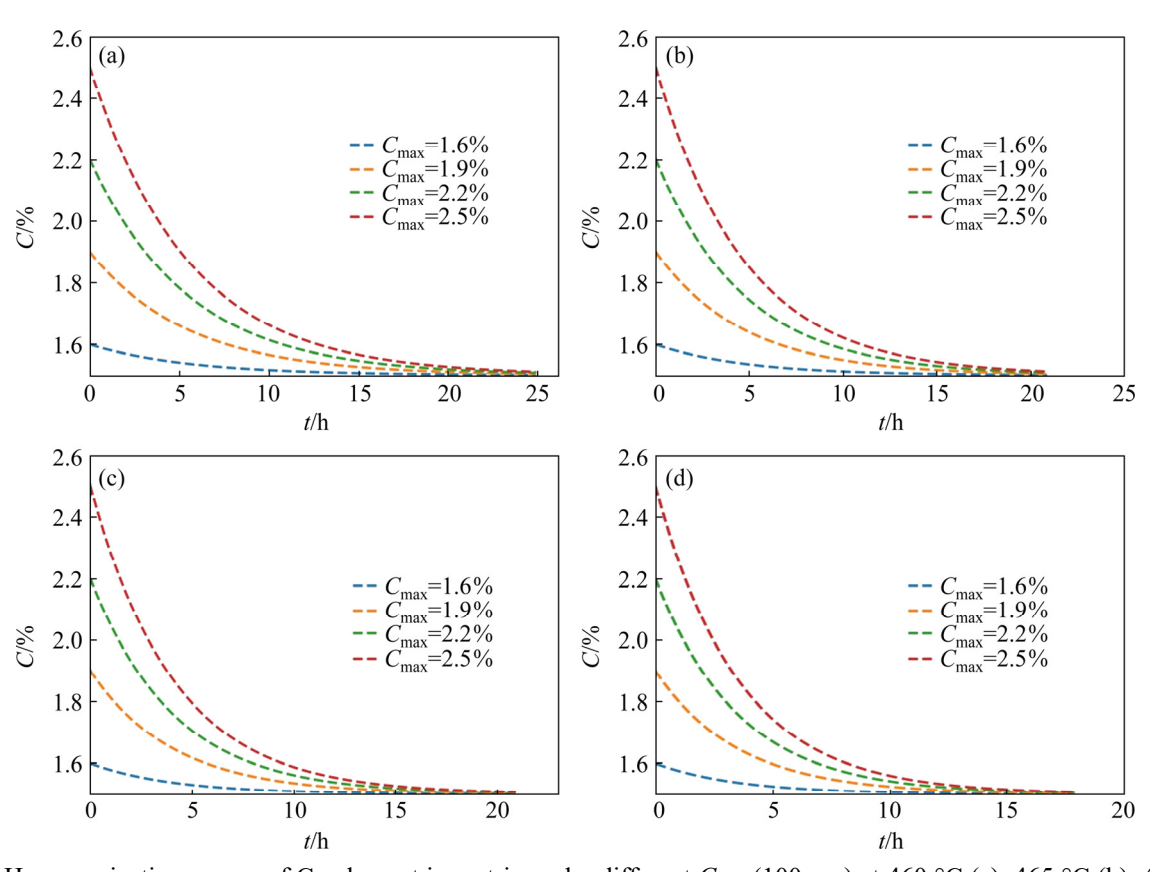


Fig. 6 Homogenization curves of Cu element in matrix under different  $C_{\text{max}}$  (100 µm) at 460 °C (a), 465 °C (b), 470 °C (c), and 475 °C (d)

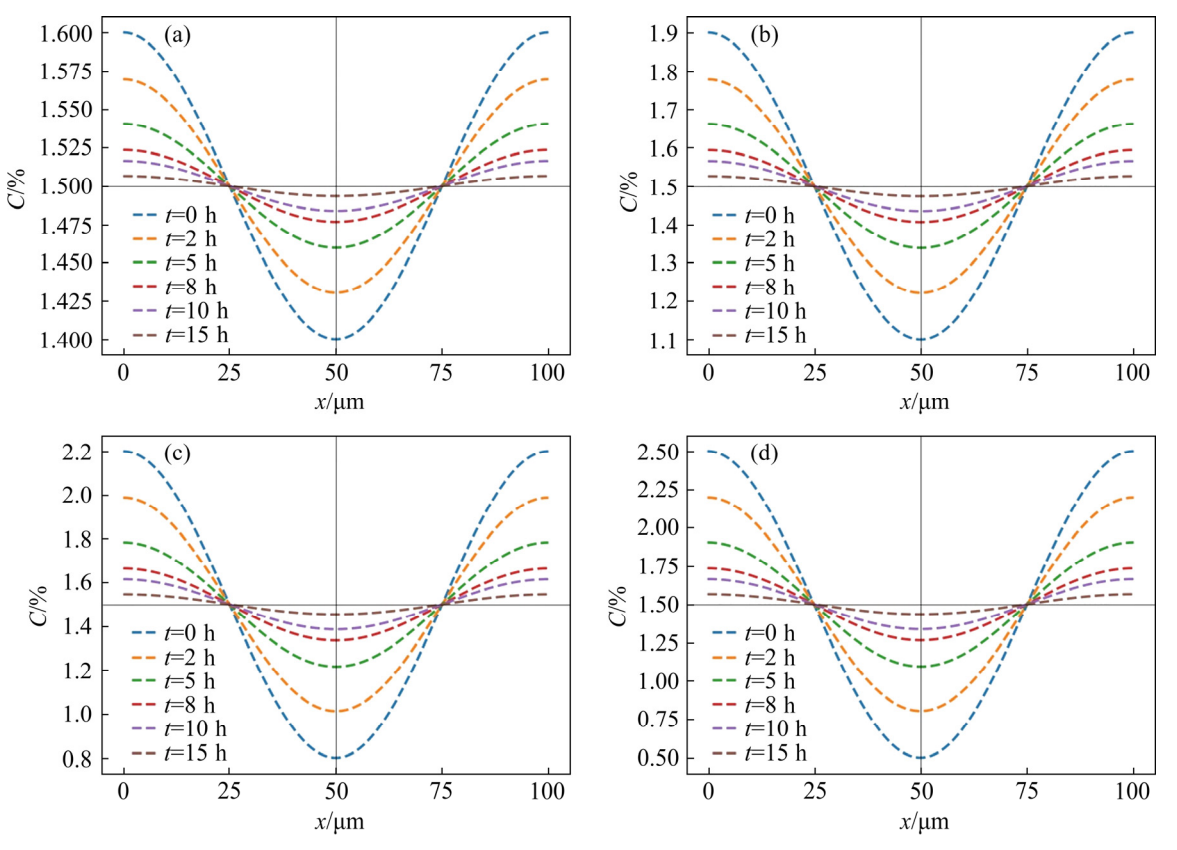


Fig. 7 Homogenization curves of Cu element in matrix at different time, 460 °C and  $C_{\rm max}$ =1.6% (a),  $C_{\rm max}$ =1.9% (b),  $C_{\rm max}$ =2.2% (c) and  $C_{\rm max}$ =2.5% (d)

In order to clarify the substantial factors affecting the concentration distribution of Cu element, it is necessary to discuss in detail different grain size conditions and different heat treatment temperature conditions. The specific results are shown in Figs. 8 and 9. When the grain size is 140 µm at 460 °C, the heat treatment time is 50 h, while when the grain size is 80 μm, the heat treatment time is only 20 h, which is enough to characterize that the grain size has a great effect on the concentration distribution of solute elements in the matrix, as shown in Fig. 8(a). When the heat treatment temperature is 475 °C, the heat treatment time is 35 h when the grain size is 140 µm, while the heat treatment time is 15 h when the grain size is 80 µm (as shown in Fig. 8(d)), which reveals that temperature only has an obvious effect on the concentration distribution in the larger grains.

Accordingly, the effects of temperature on the concentration distribution of solute elements at the same size are further compared. The results are shown more intuitively in Fig. 9, which illustrates that the effect of temperature on solute solubility distribution is based on the grain size. Combined with the above analysis, it is not difficult to find that the diffusion homogenization of solute elements in the matrix mainly depends on the grain

size.

Finally, based on the theoretical time obtained by the concentration distribution model of precipitates and solute elements, the experimental alloy was heat treated, and the evenly spaced points in the grains were analyzed by EDS. As shown in Fig. 10, the concentration distribution curve of solute elements in the grain unit is displayed, which makes it clear that the composition segregation tends to be uniform along the grain diameter direction.

#### 4 Discussion

Obtaining the best characteristics of heterogeneous microstructure, such as the collocation distribution of hard and soft micro-domains, is a prerequisite for the alloy to have both good strength and plasticity. Accordingly, controlling the distribution of precipitates and solute elements in the Al–Zn–Mg–Cu alloys determines the precise construction effect of the heterostructure in the soft and hard micro-domains, which mainly depends on the initial microstructure of the alloys and the used heat treatment conditions, such as grain size, precipitation phase size, heat treatment temperature, and time.

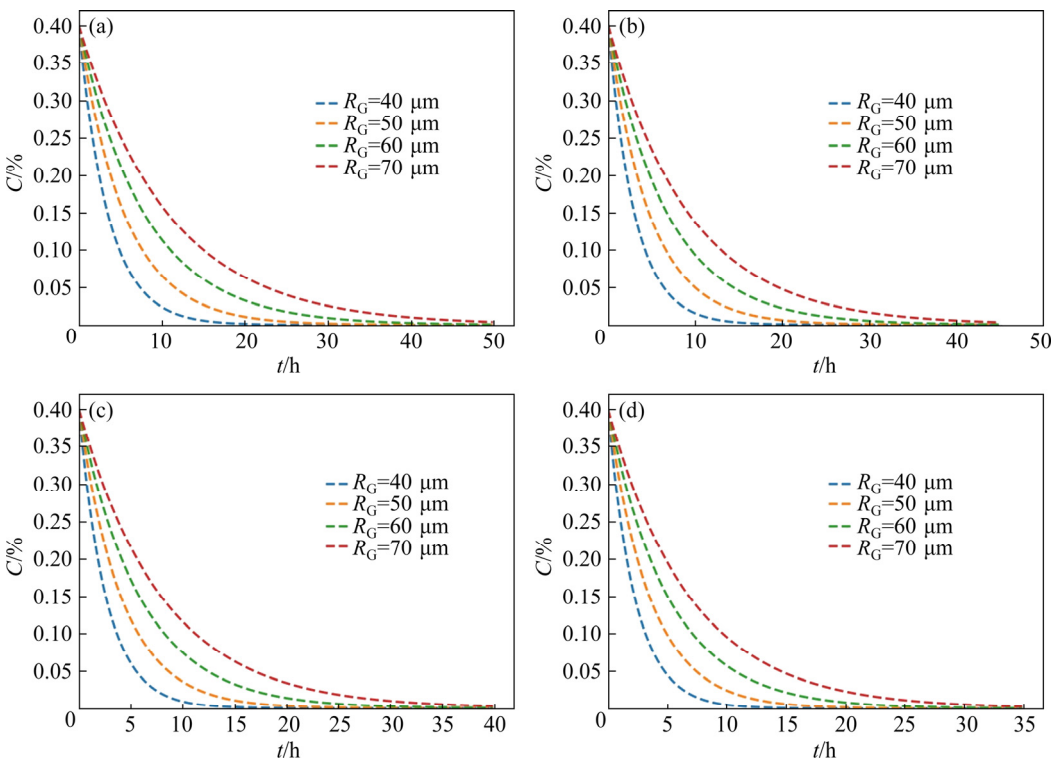


**Fig. 8** Homogenization curves of Cu element in matrix at different grain sizes and 460 °C (a), 465 °C (b), 470 °C (c), and 475 °C (d)

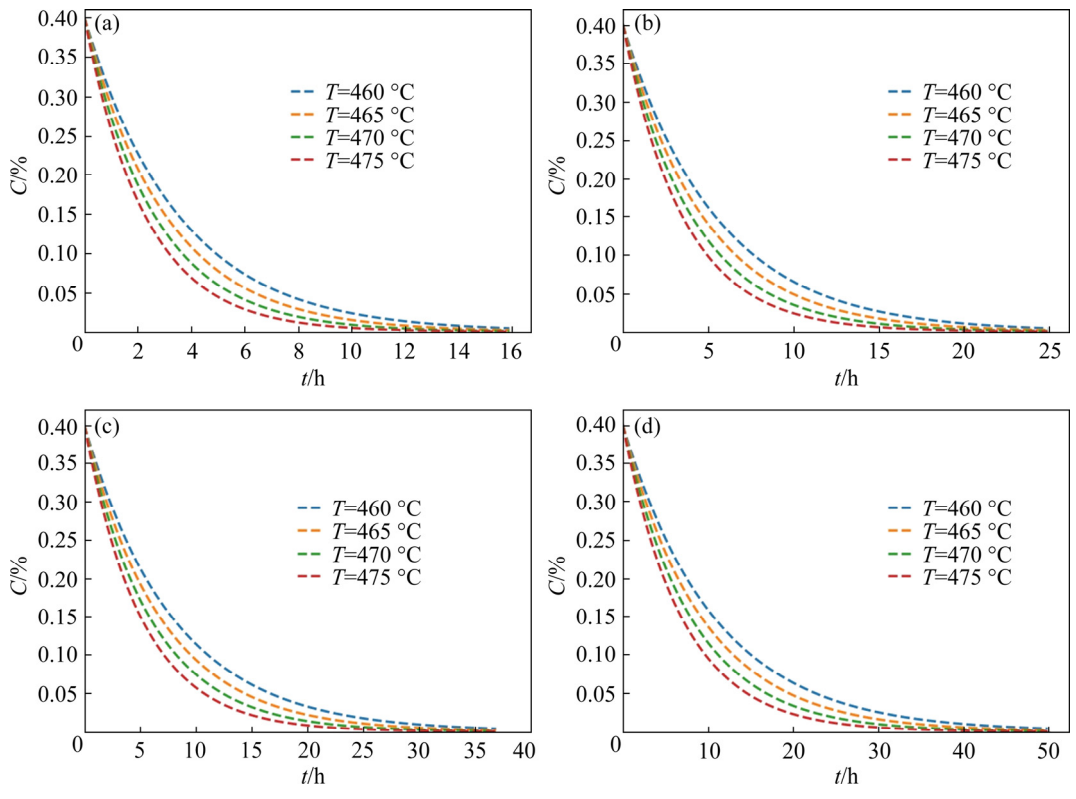
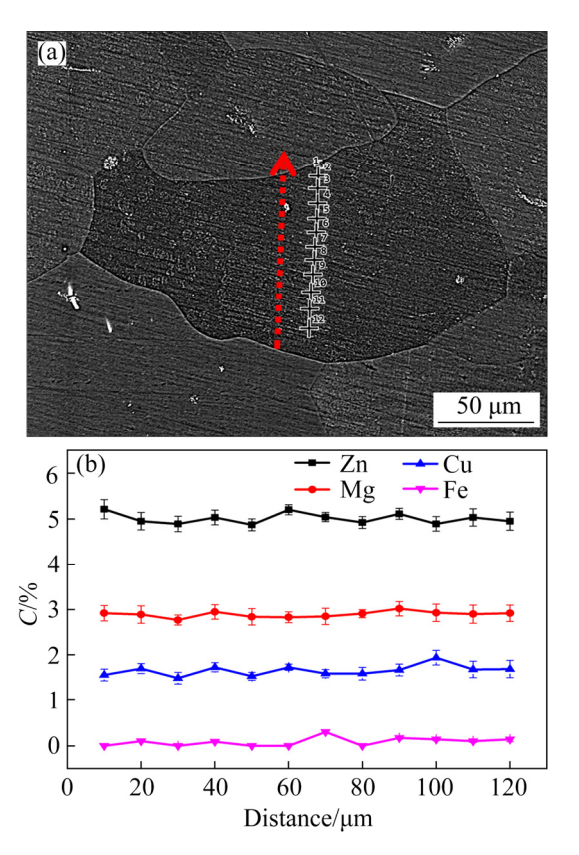


Fig. 9 Homogenization curves of Cu element in matrix at different temperatures and different  $R_G$  values of 40  $\mu$ m (a), 50  $\mu$ m (b), 60  $\mu$ m (c) and 70  $\mu$ m (d)



**Fig. 10** Microstructure and concentration distribution of solute elements in homogenized grains: (a) SEM image; (b) Concentration distribution curves

#### 4.1 Effect of initial microstructure

According to the above theoretical calculation it can be concluded that the dissolution time of the precipitates in the heat treatment process is greatly dependent on the radius of the precipitated particles. As shown in Fig. 4, the decrease in the size of the precipitates greatly shortens the dissolution time at the same heat treatment temperature. It is exciting to find that the effect of precipitate size on dissolution time remains stable with the change of heat treatment temperature, although the dissolution time of precipitates of the same size decreases with the increase of heat treatment temperature (as shown in Fig. 5). For instance, when the heat treatment is carried out at 460 °C, the dissolution time of the precipitate with a radius of 10 µm is about 4 times that of the precipitate with a radius of 5 μm, and when the heat treatment temperature 465, 470 and 475 °C, respectively, the corresponding proportional relationship between the radius of precipitated particles and dissolution time is still about 4 times. Therefore, we can naturally conclude that the dissolution time of the precipitates mainly depends on the size of the precipitates, especially the corresponding

proportional relationship is almost constant based on a certain range of heat treatment temperature. It also highlights the core effect of initial microstructure on the regulation of heterogeneous microstructure.

In the process of heat treatment, when the precipitates are dissolved, the solute elements in the matrix also diffuse along the concentration gradient, and the dissolved precipitates will promote the solute element concentration to a certain extent. Therefore, it is necessary to discuss the relationship between initial solute concentration and heat treatment time. Combined with the actual alloy composition test results, four gradient concentrations of 1.6%, 1.9%, 2.2% and 2.5% were selected to calculate the diffusion and distribution of solute element Cu in the alloy matrix with grain size of 100 µm (as shown in Fig. 6). Combined with Fig. 7, the concentration distribution trend of solute element Cu under the same initial concentration at different heat treatment time can be directly characterized. It is not difficult to find that the solute concentration in the center of the grain is relatively low, which makes the control of the solute concentration distribution in different regions become the necessary core for the formation of heterogeneous microstructure. Therefore, it is urgent to analyze and discuss the effect of different grain sizes on the regulation of heterogeneous microstructure.

Correspondingly, according to the results of Fig. 8, when the grain size is 120, 100 and 80 µm at 460 °C, the heat treatment time required for the concentration distribution of solute elements to be uniform is about 40, 30 and 20 h, respectively. It can be determined that the grain size has a very significant effect on the concentration distribution of solute elements in the matrix and the heat treatment time. In addition, it can also be found that, similar to the relationship between precipitate size and heat treatment time, the corresponding proportional relationship between grain size and heat treatment time is almost constant with the change of heat treatment temperature. Moreover, for the 140 µm grains, the corresponding heat treatment time is 50, 40 and 35 h when the heat treatment temperature is 460, 470 and 475 °C, respectively, but for the 80 µm grain, when the heat treatment temperature is 460, 470 and 475 °C, the corresponding heat treatment time is 20, 18 and

15 h, respectively, which indicates that only the larger grain size is sensitive to the change of heat treatment temperature.

In order to prepare the alloy with ideal heterogeneous microstructure, it is particularly important to control the initial size of the precipitate phases and grains. On the basis of mastering the original microstructure, the dissolution degree of the precipitates and the distribution of solute elements in the matrix can be effectively designed and adjusted by controlling the heat treatment time, so as to form different soft and hard micro-domains to accurately construct the expected heterogeneous microstructure.

#### 4.2 Effect of heat treatment conditions

There is no doubt that the heat treatment temperature has a certain effect on the dissolution of the precipitate phase and the concentration distribution of solute elements in the matrix, as shown in Fig. 5 and Fig. 9. The relationship between the heat treatment temperature and the dissolution time of the precipitate phase is based on the size of the precipitates. For example, for large-size precipitates, the reduction of heat treatment time caused by the increase of heat treatment temperature is larger than that of small-size precipitates. In other words, the effect of heat treatment temperature on large size precipitates is more significant than that of small size precipitates. Accordingly, combined with the above analysis, it can be concluded that the effect of heat treatment temperature on solute elements in large grain size is obviously higher than that in small grain size. Therefore, it is intuitive and clear that the effect of heat treatment conditions on the heterogeneous structure is based on the initial microstructure of the alloy.

For Al–Zn–Mg–Cu alloys, through the above theoretical calculation of the distribution of precipitates and solute elements, it becomes simple and feasible to form a heterogeneous microstructure with both high strength and high formability by thermomechanical treatment. The ideal initial microstructure is obtained by means of composition design and hot working process control, for instance, our previous studies have pointed out that adding Fe element to Al–Zn–Mg–Cu alloys can refine the as-cast grain size, and direct hot rolling alloy ingots can effectively break the

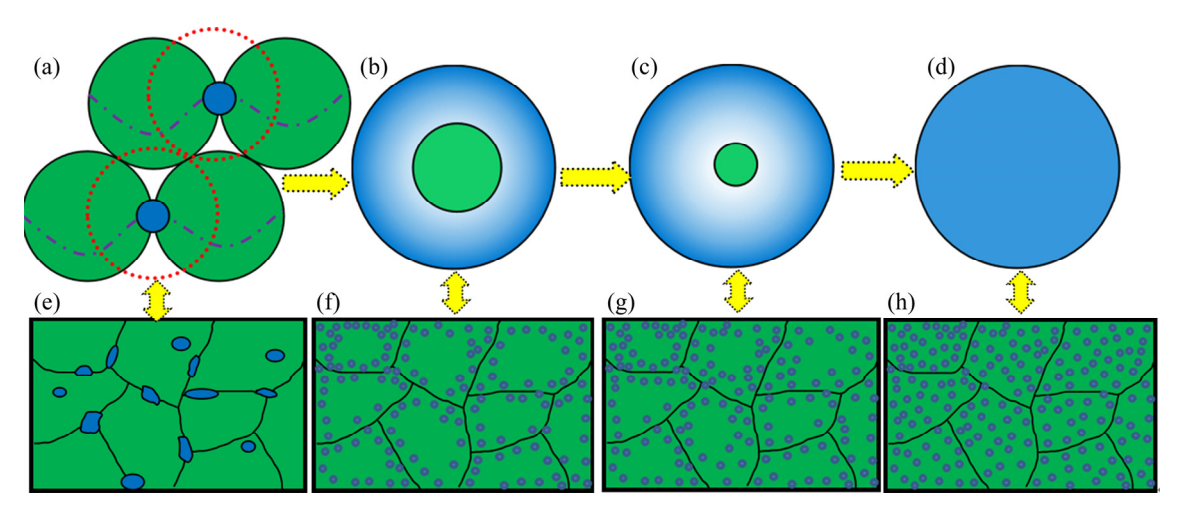


**Fig. 11** Schematic diagrams of heterogeneous microstructure formation: (a–d) Diffusion of solute elements in grain with heat treatment at 460 °C for 0, 8, 20 and 30 h, respectively; (e–h) Microstructure in alloy matrix with corresponding heat treatment at 460 °C for 0, 8, 20 and 30 h, respectively

precipitates [11,12]. After the subsequent design of effective heat treatment conditions, such as heat treatment temperature and time, and applying different degrees of heat treatment, the staggered heterostructure of soft and hard micro-domains can be obtained.

Accordingly, the schematic diagram of the formation of the heterogeneous heterostructure corresponding to the initial heterostructure of grain size of 100 µm and precipitate size of 10 µm is given. As shown in Fig. 11, according to the above calculation and analysis results, when the heat treatment is conducted at 460 °C, the microstructure evolution models of different heat treatment time are shown, i.e., the heat treatment time is 8, 20 and 30 h, respectively. The distribution of solute element Cu is indicated by blue, and the soft micro-domains with less solute element are indicated by green. Figures 11(a-d) show the diffusion of solute elements in a grain with heat treatment conditions, while Figs. 11(e-h) show the evolution of microstructure in alloy matrix with heat treatment conditions. When the heat treatment time is about 8 h, the precipitates dissolve completely and the distribution of Cu elements in the matrix reaches the maximum inhomogeneity. As shown in Figs. 11(b, f), the distribution of solute elements is relatively concentrated near the grain boundary, while there is a large soft micro-domain in the center of the grains. With the extension of heat treatment time, the area of soft micro-domain decreases gradually until the relative

distribution of solute elements in the matrix is uniform.

It can be concluded that the accurate control of heat treatment conditions based on theoretical design can effectively construct the matching degree of soft and hard micro-domains and form the expected heterogeneous structure.

#### **5** Conclusions

- (1) The dissolution process of precipitated particles in the early stage of heat treatment is mainly affected by particle size and homogenization temperature.
- (2) The diffusion homogenization process of solute elements in the matrix mainly depends on the grain size, while the heat treatment temperature only has an obvious effect on the concentration distribution in the larger grains.
- (3) The actual heat treatment results of Al–Zn–Mg–Cu alloy are in good agreement with the theoretical model predictions of precipitates and solute element concentration distribution.

#### **Acknowledgments**

This work was financially supported by the National Key Research and Development Program of China (No. 2021YFE0115900), the National Natural Science Foundation of China (Nos. 51871029, 51571023, 51301016), the Government Guided Program-Intergovernmental Bilateral Innovation Cooperation Project, China

(No. BZ2019019), and the Opening Project of State Key Lab of Advanced Metals and Materials, China (No. 2020-ZD02).

#### References

- [1] TISZA M, CZINEGE I. Comparative study of the application of steels and aluminium in lightweight production of automotive parts [J]. International Journal of Lightweight Materials and Manufacture, 2018, 1: 229–238.
- [2] GUO M X, LI G J, ZHANG Y D, SHA G, ZHANG J S, ZHUANG L Z, LAVERNIA E. Influence of Zn on the distribution and composition of heterogeneous solute-rich features in peak aged Al-Mg-Si-Cu alloys [J]. Scripta Materialia, 2019, 159: 5-8.
- [3] SCHUSTER P, ÖSTERREICHER J, KIROV G, SOMMITSCH C, MUKELI E. Characterisation and comparison of process chains for producing automotive structural parts from 7xxx aluminium sheets [J]. Metals, 2019, 9: 305.
- [4] SHIN J, KIM T, KIM D F, KIM K. Castability and mechanical properties of new 7xxx aluminum alloys for automotive chassis/body applications [J]. Journal of Alloys and Compounds, 2017, 698: 577–590.
- [5] GUO M X, ZHU J, ZHANG Y D, LI G J, ZHANG J S, ZHUANG L Z. The formation of bimodal grain size distribution in Al-Mg-Si-Cu alloy and its effect on the formability [J]. Materials Characterization, 2017, 132: 248-259.
- [6] JIANG D, PAN Q, HUANG Z. Microstructural evolution of 2026 aluminum alloy during homogenization [J]. Journal of Central South University, 2018, 25(3): 490–498.
- [7] LIU T W, WANG Q D, TANG H P, LI Z Y, LEI C, EBRAHIMI M, JING H Y, DING W J. Microstructure and mechanical properties of squeeze-cast Al-5.0Mg-3.0Zn-1.0Cu alloys in solution-treated and aged condition [J]. Transactions of Nonferrous Metals Society of China, 2020, 30(9): 2326-2338.
- [8] DUAN J, YIN Z, LEI X F. Microstructure evolution and Al<sub>3</sub>(Sc<sub>1-x</sub>Zr<sub>x</sub>) precipitates' kinetics in Al–Zn–Mg alloy during homogenization [J]. Journal of Central South University, 2013, 20: 579–586.
- [9] LIU T, HE C, LI G. Microstructural evolution in Al–Zn–Mg–Cu–Sc–Zr alloys during short-time homogenization [J]. International Journal of Minerals Metallurgy and Materials, 2015, 5: 516–523.
- [10] XIAO Q F, HUANG J W, JIANG Y G, JIANG F Q, WU Y F, XU G F. Effects of minor Sc and Zr additions on mechanical properties and microstructure evolution of AlZnMgCu alloys [J]. Transactions of Nonferrous Metals Society of China, 2020, 30(6): 1429–1438.
- [11] YUAN L L, GUO M X, ZHANG J S, ZHUANG L Z. Synergy in hybrid multi-scale particles for the improved formability of Al–Zn–Mg–Cu alloys [J]. Journal of Materials Research and Technology, 2021, 10: 1143–1157.
- [12] YUAN L L, GUO M X, YU K C, ZHANG J S, ZHUANG L Z. Multi-scale iron-rich phases induced fine microstructure in Al-Zn-Mg-Cu-Fe alloys [J]. Philosophical Magazine,

- 2021, 101: 1417–1442. VALIEV R, ALEXANDROV I, ZHU Y, LOWE
- [13] VALIEV R, ALEXANDROV I, ZHU Y, LOWE T. Paradox of strength and ductility in metals processed by severe plastic deformation [J]. Journal of Materials Research, 2002, 17: 5–8.
- [14] WANG Y F, WANG M S, YIN K, HUANG A H, HUANG C X. Yielding and fracture behaviors of coarse-grain/ultrafinegrain heterogeneous-structured copper with transitional interface [J]. Transactions of Nonferrous Metals Society of China, 2019, 29(3): 588-594.
- [15] BAE J W, MOON J, MIN J J, YIM D, KIM D, KIM D, LEE S, KIM H S. Trade-off between tensile property and formability by partial recrystallization of CrMnFeCoNi high-entropy alloy [J]. Materials Science and Engineering A, 2017, 703: 324–330.
- [16] KUMAR K S, SWYGENHOVEN H V, SURESH S. Mechanical behavior of nanocrystalline metals and alloys [J]. Acta Materialia, 2003, 51(19): 5743-5774.
- [17] MEYERS M A, MISHRA A, BENSON D J. Mechanical properties of nanocrystalline materials [J]. Progress in Materials Science, 2006, 51(4): 427–556.
- [18] MA E, ZHU T. Towards strength-ductility synergy through the design of heterogeneous nanostructures in metals [J]. Materials Today, 2017, 20(6): 323–31.
- [19] WANG Y F, WANG M S, YIN K, HUANG A H, LI Y S, HUANG C X. Yielding and fracture behaviors of coarsegrain/ultrafine-grain heterogeneous-structured copper with transitional interface [J]. Transactions of Nonferrous Metals Society of China, 2019, 29(3): 588–594.
- [20] WANG Y M, MA E. Three strategies to achieve uniform tensile deformation in a nanostructured metal [J]. Acta Materialia, 2004, 52: 1699–1709.
- [21] SHAO C W, ZHANG P, ZHU Y K, ZHANG Z J, TIAN Y Z, ZHANG Z F. Simultaneous improvement of strength and plasticity: Additional work-hardening from gradient microstructure[J]. Acta Materialia, 2018, 145: 413–28.
- [22] JO Y H, JUNG S, CHOI W M, SOHN S S, KIM H S, LEE B J, KIM N J, LEE S. Cryogenic strength improvement by utilizing room-temperature deformation twinning in a partially recrystallized VCrMnFeCoNi high-entropy alloy [J]. Nature Communications, 2017, 8: 15719.
- [23] HE J Y, WANG H, HUANG H L, XU X D, CHEN M W, WU Y, LIU X J, NIEH T G, AN K, LU Z. A precipitation-hardened high-entropy alloy with outstanding tensile properties [J]. Acta Materialia, 2016, 102: 187–196.
- [24] LYU H, HAMID M, RUIMI A, ZBIB H M. Stress/strain gradient plasticity model for size effects in heterogeneous nano-microstructures [J]. International Journal of Plasticity, 2017, 97: 46-63.
- [25] SADEGHI I, WELLS M A, ESMAEILI S. Modeling homogenization behavior of Al–Si–Cu–Mg aluminum alloy [J]. Materials & Design, 2017, 128: 241–249.
- [26] WHELAN M J. On the kinetics of precipitate dissolution [J]. Metal Science Journal, 1969, 3: 95–97.
- [27] ZUO Q, LIU F, WANG L, CHEN C F, ZHANG Z H. An analytical model for secondary phase dissolution kinetics [J]. Journal of Materials Science, 2014, 49: 3066–3079.
- [28] ROMETSCH P A, ARNBERG L, ZHANG D L. Modelling dissolution of Mg<sub>2</sub>Si and homogenisation in Al–Si–Mg

- casting alloys [J]. International Journal of Cast Metals Research, 1999, 12(1): 1–8.
- [29] ZHANG X K, GUO M X, ZHANG J S, ZHUANG L Z. Dissolution of precipitates during solution treatment of Al-Mg-Si-Cu alloys [J]. Metallurgical and Materials Transactions B, 2016, 47: 608-620.
- [30] WANG S H, MENG L G, YANG S J, FANG C F, HAO H, DAI S L, ZHANG X G. Microstructure of Al–Zn–Mg–Cu– Zr–0.5Er alloy under as-cast and homogenization conditions [J]. Transactions of Nonferrous Metals Society of China, 2011, 21(7): 1449–1454.
- [31] ZHANG C S, ZHANG Z G, LIU M. Effects of single and multi-stage solid solution treatments on microstructure and

- properties of as-extruded AA7055 helical profile [J]. Transactions of Nonferrous Metals Society of China, 2021, 31(7): 1885–1901.
- [32] GUO M X, ZHANG Y D, LI G J, JIN S B, SHA G, ZHANG J S, ZHUANG L Z, LAVERNIA E J. Solute clustering in Al–Mg–Si–Cu–(Zn) alloys during aging [J]. Journal of Alloys and Compounds, 2019, 774: 347–363.
- [33] DU Y, CHANG Y A, HUANG B Y, GONG W P, JIN Z P, XU H H, YUAN Z H, LIU Y, HE Y, XIE F Y. Diffusion coefficients of some solutes in fcc and liquid Al: Critical evaluation and correlation [J]. Materials Science Engineering A, 2003, 363: 140–151.

### Al-Zn-Mg-Cu 合金异构组织内沉淀和 溶质分布的理论设计和过程调控

袁亮亮<sup>1</sup>, 郭明星<sup>1,2</sup>, 鄢 勇<sup>3,4</sup>, 冯伟俊<sup>3,4</sup>, 刘赞扬<sup>1</sup>, 庄林忠<sup>1,2</sup>

- 1. 北京科技大学 新金属材料国家重点实验室, 北京 100083;
- 2. 北京科技大学 北京现代交通金属材料与加工实验室, 北京 100083;
- 3. 宝山钢铁股份有限公司 宝钢中央研究院 宝武铝业技术中心, 上海 201900;
  - 4. 中国宝武钢铁集团 三门峡铝基新材料研发中心, 山门峡 472099

摘 要:为了同时提高 Al-Zn-Mg-Cu 合金强度和成形性能,构建析出相和溶质元素浓度分布理论模型,并对合金内异构组织进行理论设计和过程调控。研究结果表明,沉淀相的溶解主要受其尺寸和热处理温度影响,溶质元素在合金基体中扩散所形成的异构组织特征主要取决于晶粒尺寸,而热处理温度仅对较大尺寸晶粒内的溶质元素浓度分布有显著影响。上述理论预测 Al-Zn-Mg-Cu 合金内的沉淀相和溶质元素分布情况与实测结果较为吻合。此外,通过有效控制 Al-Zn-Mg-Cu 合金内沉淀相和溶质元素浓度分布可以更好地精准构筑微区异构组织,从而更大幅度地改善合金的成形性能。

关键词: Al-Zn-Mg-Cu 合金;浓度分布;扩散;异构组织;模型

(Edited by Wei-ping CHEN)